Quantum Statistical Corrections to Dynamic Nuclear Magnetic Resonance

Leonard J. Mueller and Daniel P. Weitekamp*

A quantum statistical treatment of the chemical exchange between molecular eigenstates or conformations revealed previously unsuspected dynamic terms in the spin Hamiltonian operator that describes fast exchange. These terms resulted from the effect of nuclear spin on rotational and vibrational relaxation. With the traditional theory, an interpretation of new carbon-13 nuclear magnetic resonance measurements of the chemical shift of methylcyclohexane in solution showed fast-exchange equilibrium constants that were inconsistent with the slow-exchange free-energy difference and were spread over a range of 30 percent for the various carbon-13 positions. Modeling of the new terms indicated that they have the correct magnitude and temperature dependence to reconcile these inconsistencies.

Almost all magnetic resonance experiments are performed on molecules undergoing rotational and vibrational (rovibrational) rate processes that are sufficiently rapid to affect the line shape. The signatures of the chemical exchange between rovibrational states or between conformers (subsets of rovibrational states that are associated with a particular minimum of the potential energy) include line broadening, coalescence of lines, and exchange narrowing to line positions corresponding to a temperature-dependent spin Hamiltonian. The resulting line shapes provide quantitative conformational probabilities and rates of interconversion and thus provide information on the molecular potentials that underlie kinetic and equilibrium properties. For five decades, increasingly general theoretical formalisms have been proposed and applied to the interpretation of these dynamic magnetic resonance spectra (*1–6*). A key approximation in these traditional theories, which was stated in the seminal work (*1*), is to neglect the reaction of the spins on the rapidly relaxing spatial degrees of freedom. An earlier attempt to remove this approximation with a static equilibrium description of the fast-exchange spin Hamiltonian (*7*) resulted in the unsuccessful fitting (*6, 8*) of various experimental results with two-state models of the rapidly relaxing degrees of freedom and in the conclusion that the traditional theory was adequate. However, our experiments demonstrated that the traditional assumptions underlying dynamic nuclear magnetic resonance (NMR) are untenable and motivated a reexamination of the approximations that have been made.

In our study, we included the back action of spin on the rapidly relaxing degrees of freedom within a dynamic system-bath formalism, which was similar to that widely used (*1–6, 9*) to treat thermally modulated spin Hamiltonians. Our focus was on the much stronger (but spin-independent) fluctuations that are responsible for chemical exchange. We found that the fast-exchange magnetic resonance line positions were strongly affected by details of the rovibrational rate processes through previously unsuspected contributions to the spin Hamiltonian, which is linear (*10*) in each nuclear spin moment. Omitting these terms and using only equilibrium statistical mechanics of the system (the rovibrational and spin degrees of freedom of the target molecule) introduced systematic errors. These insights were applied to resolve large apparent inconsistencies in new dynamic ^{13}C measurements.

We made these improved (*11–13*) measurements on the well-studied system of methylcyclohexane in solution because this system is reportedly consistent with the traditional theory (*8, 14, 15*). Methylcyclohexane is favorable for studying chemical exchange because of its five inequivalent carbon sites (Fig. 1) and its long liquid state temperature range over which the rate of conformer interconversion varies rapidly. At 11.7 T, the ^{13}C NMR spectrum of methylcyclohexane (*16*) in solution at 160 K (Fig. 2) illustrates the slow-exchange regime. In this regime, barrier crossing at rates that are slow in comparison with the differences between the conformers' spin resonance frequencies leaves resolved spectral lines for each of the two conformers. The distinct resonances that result from the dominant equatorial conformation are apparent (Fig. 2). The much smaller signal from the methyl carbon (C-Me) position of the axial conformer is shown on an expanded scale (Fig. 2, inset), and the C-2,6 and C-3,5 axial conformers are similarly well resolved. The C-1 axial resonance overlaps with the equatorial C-3,5 peak but was resolved in the present work with the distortionless enhancement of polarization technique (DEPT) spectral editing experiment (*11*). For C-4, the axial and equatorial resonances are degenerate, and the single spectral line is not broadened throughout the entire range of chemical exchange. We used this line as an internal chemical shift reference.

The areas of the individual conformer lines were used to measure the equilibrium probability ratio $K = p^{ax}/p^{eq}$ (K, equilibrium constant; p^{ax}, probability of the axial conformation; p^{eq}, probability of the equatorial conformation) at temperatures between 145 and 190 K, allowing a determination of the difference ΔA in conformer Helmholtz (constant volume) free energies of the form

$$\Delta A(T) = \Delta A_0 + T d\Delta A(T)/dT = -RT \ln K(T) \qquad (1)$$

where T is absolute temperature and R is the gas constant. The best fit parameters ($\Delta A_0 = 6956 \pm 140$ J mol^{-1} and $d\Delta A(T)/dT = 3.12 \pm 0.81$ J mol^{-1} K^{-1}) are highly correlated, with a covariance of 113 (*17*).

To interpret the fast-exchange line positions, we extrapolated the chemical shifts of each conformer to the higher fast-exchange temperatures. Methylcyclohexane is favorable because of the certainty with which this extrapolation may be performed (*18*). Over the range of slow-exchange temperatures, the chemical shifts exhibit a linear dependence on temperature that differs from site to site. The internally referenced values $\Delta\nu_i = \nu_i - \nu_4$ are described by the form

$$\Delta\nu_i = m_i T + b_i \qquad (2)$$

where the slopes m_i and intercepts b_i are,

Fig. 1. The equatorial and axial conformations of methylcyclohexane. The carbon sites are labeled.

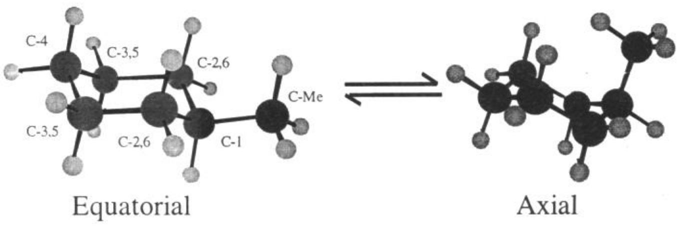

A. A. Noyes Laboratory of Chemical Physics, 127-72, California Institute of Technology, Pasadena, CA 91125, USA.

*To whom correspondence should be addressed. E-mail: weitekamp@caltech.edu

within measurement error, the same as those resulting from the global fit of Table 1.

As the temperature is raised, the resolved conformer resonances broaden, coalesce, and collapse into a single line for each distinct carbon position. The traditional theory predicts that the fast-exchange line positions can be calculated from the weighted average of the spin Hamiltonians of the conformers. In the present context, this reduces to

$$\Delta\nu_i^{\mathrm{fast}} = p^{\mathrm{eq}}(T)\Delta\nu_i^{\mathrm{eq}}(T) + p^{\mathrm{ax}}(T)\Delta\nu_i^{\mathrm{ax}}(T) \qquad (3)$$

One prediction of the traditional theory is that the data for the various carbon sites should result in the same conformer probabilities, assuming (as in Eq. 3) negligible isotope effects of the ^{13}C placement on the equilibrium constant. The test of this prediction is shown in Fig. 3. With the conformer shifts determined by the slow-exchange chemical shifts that were extrapolated linearly to higher temperatures (Eq. 2), the conformer probabilities were calculated (with Eq. 3) from the observed fast-exchange line positions for each of the four sites that have resolved conformer lines. The resulting apparent equilibrium constants are spread over a 30% range for the various carbon positions (Fig. 3)—either there is a very large isotope effect on K or this widely used procedure is internally inconsistent. Because the determination of K from the ratio of line areas in the slow-exchange regime is consistent (within measurement error) with a single equilibrium constant for the different isotopomers, we conclude that the traditional procedure is inconsistent. The fast-exchange line positions can also be predicted with Eq. 3 and a linear extrapolation of the slow-exchange chemical shifts (Eq. 2) and free-energy difference (Eq. 1). The resulting frequencies deviate by up to 8 Hz from the observed fast-exchange line positions.

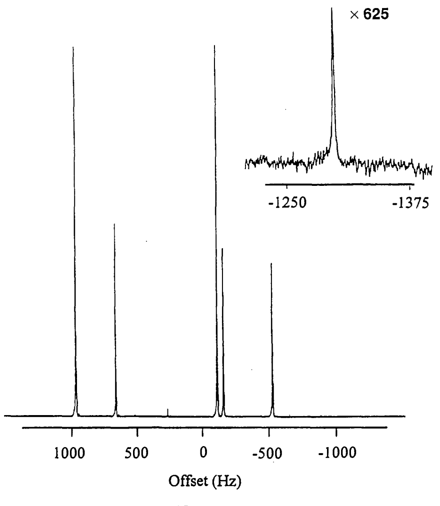

Fig. 2. The 11.7-T ^{13}C NMR spectrum of methylcyclohexane at 160 K. The inset, with vertical scale magnified by 625, shows the much smaller signal from the C-Me position of the axial conformer.

These observations show the failure of the traditional theory to provide structural information from fast-exchange spectra at a high level of accuracy, which is expected and often assumed. The magnitude of this failure is better quantified with global fits to the entire data set with the reduced χ^2 statistic (*19*). For the model consisting of Eqs. 1 through 3 with a single pair of thermodynamic parameters [ΔA_0 and $d\Delta A(T)/dT$] for all conformers, the reduced χ^2 for the global fit is 22. Including quadratic and cubic terms in the temperature dependence of ΔA hardly improves the fit ($\chi^2 = 20$). Assuming random errors only (*20*), we excluded both models with essentially complete certainty.

The traditional theory posits that the only effect of the rapid turmoil of motional averaging is to supply spin-independent rates for transporting the molecules between spatial states. To derive equations of motion for the spins from first principles, we adapted the second-order weak-collision theory for a system coupled to a quantum mechanical thermal reservoir or bath (*21*). The system-bath coupling Hamiltonian (V) appears quadratically in complex-valued spectral densities, which are the constants in the reduced equations of motion that describe the time dependence of the system. A key step is to define the system as consisting of molecular eigenstates of both spin and spatial interactions, such as those that are shown in the double-well model (Fig. 4), where the manifold of spatial (rovibrational) states within each conformer well is shown to be split according to (exaggerated) spin energies. The bath may be envisioned as the solvent along with any intramolecular degrees of freedom that are not modeled as the system. The Hamiltonian V, which is responsible for the rovibrational relaxation, is spin independent. With these ingredients, a formal microscopic description (*22*) was made of the time dependence of a spin coherence within this system in the presence of rovibrational relaxation.

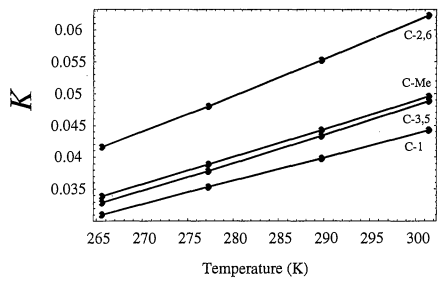

Fig. 3. The inconsistency of conformer equilibrium constants (K) as determined with traditional assumptions. Interpretation of fast-exchange line positions with a linear extrapolation of conformer chemical shifts from the slow-exchange data shows a large apparent dependence of K on the position of ^{13}C. The error bars on the data are on the order of 0.5% of the equilibrium constant and are too small to be seen at this scale.

The coherence of interest is between system states $|m\rangle$ and $|m'\rangle$, which differ only in spin state. The elementary step in the rovibrational relaxation process is a thermal rate process (between, say, system state $|k\rangle$ and system state $|m\rangle$) that conserves the spin state. A dynamic frequency shift Δ_{mkkm}) is associated with each microscopic contribution J_{mkkm}) to this rate. These two quantities are not independent; instead, they form a Hilbert-transform pair (*21*) with respect to the energy that the bath must exchange with the system for the rate process to occur. Including the spin interactions as one contribution to this energy has two important effects. The first is that the resulting equations of motion bring the system to equilibrium—a test that the traditional theory fails (*7*). The second and more important effect is that the rovibrational dynamic frequency shifts, which are evaluated at system Bohr frequencies that include spin, now appear in the equations of motion for spin evolution. Specifically, the unitary evolution of spin coherence between states $|m\rangle$ and $|m'\rangle$ experiences a novel type of dynamic frequency shift

$$\Delta^{m'm} = \sum_k [\Delta_{m'kkm'}(\omega_{km'}) - \Delta_{mkkm}(\omega_{km})] \qquad (4)$$

where ω_{km} is the system Bohr frequency at which energy is exchanged with the bath in an elementary step of the thermal relaxation.

For the case of interest, where $|m\rangle$ and $|m'\rangle$ differ only in spin state, the sum over other rovibrational levels (k) can be grouped by the spin state as well, because V does not connect different spin states. Thus, Eq. 4 is a sum over rovibrational levels of differences in the imaginary component of the spectral density evaluated at two Bohr frequencies that differ only by the contribution of spin energy (for example, the difference in chem-

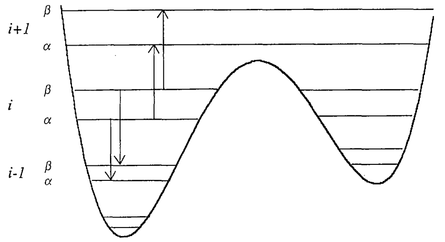

Fig. 4. Schematic of a multistate model for chemical exchange. A ladder of spin-conserving rovibrational transitions (connecting spatial state i to states $i \pm 1$) models barrier crossing and motional-averaging effects on coherences between spin states (labeled α and β). Level spacing is not to scale.

ical shift) to the total energy that must be provided by the bath for the rate process to occur. The energy dependence of the rovibrational dynamic frequency shifts in these purely spatial rate processes results in different shifts for different spin states. Thermodynamics demands that the thermal rates must on average respect the existence of spin energies, including the small energy difference of a given spin state in different rovibrational states. Causality demands that we include the shifts in energy that accompany the rate processes. This is the origin of the new terms in the spin Hamiltonian parameters, which we refer to as ALBATROSS (average Louvillian born as the result of spatial susceptibility) terms (*23*).

Because of the large disparity in spatial and spin frequencies and the relative insensitivity of experiments to initial conditions and rates, the dependence of J_{mkkm} (but not Δ_{mkkm}) on spin energy will typically be numerically unimportant. Making this simplification gives the equation of motion for the system density operator $\sigma(t)$ as

$$\langle m'|\dot{\sigma}(t)|m\rangle = -\left\{ i(\omega_{m'm} + \Delta^{m'm}) + \sum_{n'} W_{m'n'} \right\} \langle m'|\sigma(t)|m\rangle + \sum_{n'} W_{n'm'} \langle n'|\sigma(t)|n\rangle \tag{5}$$

where $W_{m'n'}$ is the total rate from the rovibrational state associated with label m' to that associated with the label n', with spin dependence neglected. This form is similar to the traditional equations of motion for the spin coherence, with the only difference being the newly recognized ALBATROSS shifts $\Delta^{m'm}$.

An even simpler notation is obtained by renaming $\Delta^{m'm}$ as Δ_i, where i is the common spatial label of the two states in spin superposition. The observed chemical shift in the fast-exchange limit can be written as the sum of the traditional (trad) expression and the population-weighted ALBATROSS (ALB) shifts, which are summed over rovibrational states

$$\langle\omega\rangle = \sum_{i = A,B,C\ldots} p_i(\omega_i + \Delta_i) = \langle\omega\rangle_{\mathrm{trad}} + \langle\omega\rangle_{\mathrm{ALB}} \tag{6}$$

Because the important terms in Eq. 6 can be divided into subsets that correspond to conformers, it is possible that the two-site form of Eq. 3 is usable. However, the chemical shifts of each conformer are rate-dependent. This aspect makes them fundamentally different from the traditional concept of a Boltzmann average $\langle\omega\rangle_{\mathrm{trad}}$ of system eigenvalues.

The modeling of the ALBATROSS shift is complicated because of its dynamic character and because it can emphasize states that are different from those that dominate the traditional term. The rovibrational states with relatively large ALBATROSS shifts are those that are connected by large rates to states with large differences in spin Hamiltonians. Energetically close states with different spin Hamiltonians also characterize systems with a large temperature dependence of the traditional contribution to the fast-exchange average.

Table 1. Best fit parameters for the temperature dependence of the ALBATROSS shift and chemical shifts of the equatorial and axial sites in methylcyclohexane.

Carbon atom	Equatorial		Axial		ALBATROSS shift	
	Slope (Hz K^{-1})	Intercept (Hz)	Slope (Hz K^{-1})	Intercept (Hz)	Linear (Hz K^{-1})	Quadratic (Hz K^{-2})
C-Me	−0.47514	−287.73	−0.24347	−1095.75	−0.03005	−0.00008687
C-1	0.00191	833.71	−0.07757	158.21	−0.02896	0.00020918
C-2,6	0.26748	1087.09	0.19754	657.65	−0.07534	−0.00001764
C-3,5	0.04618	39.86	−0.02021	−706.92	−0.05220	0.00006580

Evidently, a general approach to modeling dynamic NMR must involve multistate descriptions of the exchange coordinate, which include the dependence of the spin Hamiltonian on energy and (the qualitatively new feature) the detailed dynamics as a function of temperature, even in the fast-exchange limit. This complicates the analysis of dynamic NMR data far beyond the traditional analysis by greatly increasing its kinetic complexity and by suggesting that a link to the molecular dynamics of intermolecular interaction may be necessary to replace the impractical task of realistically modeling the solvent quantum mechanically.

We modeled the ALBATROSS term of the chemical shift with a multistate double-well model, which is schematically illustrated in Fig. 4. The double-well depths, the barrier height, and the rates of barrier crossing are close to those of methylcyclohexane. The rovibrational relaxation connecting adjacent levels was modeled as originating from a single off-diagonal perturbation (V) with an exponential autocorrelation time of 10^{-14} s and a matrix element whose square increases linearly with energy, which is similar to a harmonic oscillator relaxed by a thermalized perturbation linear in its displacement. The chemical shift was taken to vary as a cubic function of energy above the bottom of each well. The resulting temperature-dependent ALBATROSS shift is shown in Fig. 5. A supralinear activation of the ALBATROSS shift with temperature is found between the regimes that are characteristic of slow and fast exchange, and it reproduces (with plausible parameters) the order of magnitude (several hertz) of the discrepancy between the traditional theory and the experimental data on methylcyclohexane. Modeling in greater detail with the present formalism will require input from theory on the system density of states, the state dependence of the chemical shift, and the microscopic rates.

The multistate model suggests that the discrepancy between our experiment and the traditional procedure for relating slow- and fast-exchange spectra is associated with the activated nature of the ALBATROSS terms, which follows from the origin of the terms in the rate processes. This reasoning motivates a new fit with the simplifying assumption that, for each site, the ALBATROSS shift can be approximated by an additional quadratic function of temperature and constrained to become negligibly small near the start of intermediate exchange (200 K) and then extend only into the fast-exchange region. A

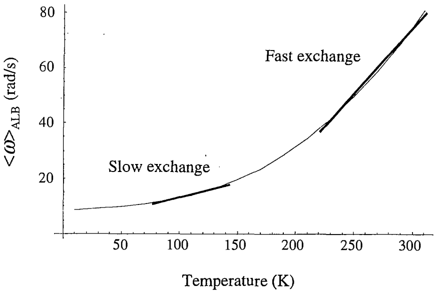

Fig. 5. A multistate calculation of the ALBATROSS shift as a function of temperature (thin curve). The thick black lines indicate the temperature ranges of high-resolution line shapes. The plotted quantity for fast exchange is $\langle\omega\rangle_{\mathrm{ALB}}$ of Eq. 6. For slow exchange, it is this quantity with the sum over states restricted to states in the lower well. The spectral density results from an autocorrelation time of 10^{-14} s for the system-bath coupling Hamiltonian V and setting $|V^2|$ to give an exchange rate of 5.88 s^{-1} from the B to the A conformer manifolds at 150 K. Each conformer well has 10 equally spaced rovibrational states with an energy difference of 4847 J mol^{-1} within the A conformer manifold and a spacing of 4098 J mol^{-1} within the B conformer manifold. The chemical shift of the A conformer manifold increases as a cubic function of energy from zero to the transition state value of 10^4 rad s^{-1} (13 parts per million), and the chemical shift of the B conformer manifold increases similarly from 10^3 rad s^{-1} to this transition state value. The relaxation rates between the nearest neighboring rovibrational states increase linearly with the state energy.

model with a linear temperature dependence of a single conformer free-energy difference regardless of ^{13}C position (Eq. 1), a linear temperature dependence of the chemical shifts of the slow-exchange conformer (Eq. 2), and a quadratic ALBATROSS shift that is unique to each site gives an excellent fit to the data with a reduced χ^2 of 1.05, which is well within the 95% confidence limit. The fast-exchange data are shown with the best fit to this model (Fig. 6); the site-specific parameters are presented in Table 1. In this fit, all carbon sites share a single conformer free-energy difference of ΔA_0 = 6966 J mol^{-1} and $d\Delta A(T)/dT$ = 3.05 J mol^{-1} K^{-1} over the range from 145 to 300 K. These thermodynamic values, as well as the linear coefficients of temperature dependence, are consistent with the same parameters extracted from the slow-exchange data only. The statistics show that this fit (and any satisfactory theory for the present data) should be accurate to a few hundredths of a hertz. Any such fit requires contributions to the chemical shift with a temperature dependence that is much greater than that measured in slow exchange. Because the ALBATROSS terms from the multistate modeling have this character and are two orders of magnitude greater than the experimental precision, it appears that ALBATROSS must be a part of any such theory.

The common procedure of extrapolating conformer spin Hamiltonians linearly with temperature has no theoretical basis, and most chemical-exchanging systems are less favorable than methylcyclohexane for experimentally testing this linearity. The ALBATROSS shift may be an important contribution to the temperature dependence of the spin Hamiltonian within a conformer, but it will contribute more strongly at the higher rates associated with intermediate and fast exchange. The present theory explains why linear extrapolation is expected to fail over a temperature range where rates are rapidly activated, but ALBATROSS is not necessarily the only important contribution to such a nonlinearity.

The multistate modeling and successful global fit with shifts that are activated in intermediate exchange provide hope that the new physics presented will be a key ingredient in calculating NMR line positions to the accuracy with which they can be measured. Although more extensive and realistic modeling is needed to make quantitative predictions, it appears from modeling at the present level that this system is not atypical. Preliminary simulations for the cases of determining rotamer populations (by way of fast-exchange *J* couplings) or nuclear hyperfine couplings (by way of paramagnetic shifts due to rapidly relaxing electron spins) indicate that a neglect of ALBATROSS contributions in the interpretation will frequently result in errors in the first significant digit. Such discrepancies would typically exceed the errors that were due to experimental accuracy. The new equations of motion give intermediate-exchange linewidths that are very similar to those of the traditional theory, and therefore, previously reported conformer interconversion rates and activation barriers are not likely to be as significantly affected. Analogs of ALBATROSS shifts may be important in the interpretation of spectral parameters in other spectroscopic contexts where motional narrowing occurs.

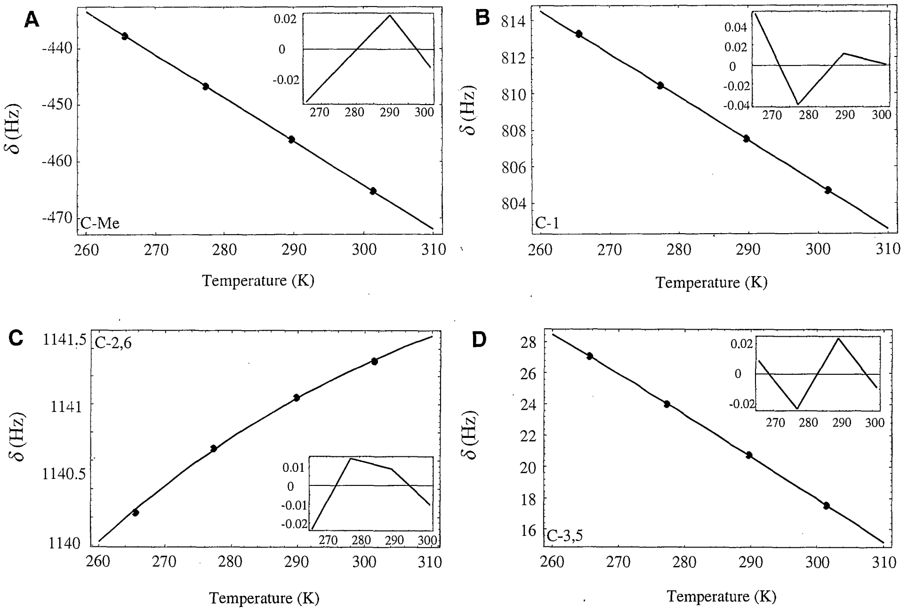

Fig. 6. Fast-exchange line positions and best global fits motivated by ALBATROSS. The carbon sites are (**A**) C-Me, (**B**) C-1, (**C**) C-2,6, and (**D**) C-3,5. Shifts (δ) are measured in relation to C-4, and the insets show the residuals. The four carbon sites share a single conformer free energy difference of ΔA_0 = 6966 J mol^{-1} and $d\Delta A(T)/dT$ = 3.05 J mol^{-1} K^{-1} over the entire temperature range from 145 to 300 K. Other fit parameters are in Table 1.

References and Notes

1. N. Bloembergen, E. M. Purcell, R. V. Pound, *Phys. Rev.* **73**, 679 (1948).
2. E. L. Hahn and D. E. Maxwell, *ibid.* **88**, 1070 (1952); H. S. Gutowsky, D. W. McCall, C. P. Slichter, *J. Chem. Phys.* **21**, 279 (1953); H. M. McConnell, *ibid.* **28**, 430 (1957); S. Alexander, *ibid.* **37**, 967 (1962); C. S. Johnson, *ibid.* **41**, 3277 (1964); R. M. Lynden-Bell, *Prog. Nucl. Magn. Reson. Spectrosc.* **2**, 163 (1967); A. J. Vega and D. Fiat, *J. Magn. Reson.* **19**, 21 (1974); S. Szymanski, M. Witanowski, A. Gryff-Keller, *Annu. Rep. NMR Spectrosc.* **8**, 227 (1978).
3. L. G. Werbelow, *J. Chem. Phys.* **70**, 5381 (1979).
4. L. Werbelow and R. E. London, *Concepts Magn. Reson.* **8**, 325 (1996).
5. G. Binsch and H. Kessler, *Angew. Chem.* **19**, 411 (1980); J. Jeener, *Adv. Magn. Reson.* **10**, 1 (1982).
6. K. E. O'Hara and C. T. Slichter, *J. Magn. Reson. Ser. A* **109**, 74 (1994); E. R. Johnston, J. S. Barber, M. Jacomet, J. C. Barborak, *J. Am. Chem. Soc.* **120**, 1489 (1998).
7. D. H. Jones, N. D. Kurur, D. P. Weitekamp, *Bull. Magn. Reson.* **14**, 214 (1992).
8. F. A. L. Anet and D. I. Freedberg, *Chem. Phys. Lett.* **208**, 187 (1993).
9. A. G. Redfield, *Adv. Magn. Reson.* **1**, 1 (1965); A. Abragam, *Principles of Nuclear Magnetism, International Series of Monographs on Physics* (Clarendon, Oxford, ed. 1, 1961).
10. The new terms here are distinct from dynamic frequency shifts that have been described earlier for the very different case where the fluctuating perturbation is a spin Hamiltonian (*3, 4*). In the current experiments, this type of mechanism is negligible. For a single ^{13}C spin with a Larmor frequency of 125 MHz and a spin-lattice relaxation time T_1 of 1 s due to a fluctuation with a (rotational) correlation time of 10^{-10} s, the previously known mechanism (*4*) would introduce a shift of only 0.013 Hz, which is more than two orders of magnitude smaller than the experimental and calculated effects that are of interest here. The previously known dynamic frequency shifts are quadratic in the spin interactions, whereas the new dynamic terms are linear in the spin interactions.
11. D. M. Doddrell, D. T. Pegg, M. R. Bendall, *J. Magn. Reson.* **48**, 323 (1982).
12. G. A. Morris, *ibid.* **80**, 547 (1988).
13. A. L. Van Geet, *Anal. Chem.* **42**, 679 (1970).
14. V. J. Basus, thesis, University of California, Los Angeles (1975).
15. M. E. Squillacote and J. M. Neth, *Magn. Reson. Chem.* **25**, 53 (1987).
16. All measurements were performed with a 500-MHz (proton Larmor frequency) commercial spectrometer on a single sample that consisted of a 2:1:1 mixture by volume of methylcyclohexane with ^{13}C in natural abundance, CS_2, and toluene-d_8. This mixture was ~4 M in methylcyclohexane, and the 5-mm sample tube was sealed under vacuum. The low-temperature spectra were obtained with DEPT (*11*) and processed by deconvolving a line shape to remove the effect of magnet inhomogeneity (*12*), zero filling once, and applying a 1-Hz exponential filter. The C-1 axial resonance was resolved from the C-3,5 equatorial resonance by varying the final pulse flip angle in the DEPT experiment and combining the data sets appropriately. The peak area and frequency were extracted by nonlinear least squares fitting, and the errors in the fits were determined by calculating the covariance matrix with the noise seen in raw Fourier transform spectra (no line-shape correction, zero filling, or exponential filter). For the peak areas and axial peak positions, these errors were used in the χ^2 analysis for the free energy and chemical shift temperature dependence. The extracted error bars on the equatorial line positions were much smaller than an apparent 0.02 to 0.04 Hz instability of the spectrometer. This unexpected source of error was included by

increasing the error bars on the line positions to give a χ^2 value of 1 and then calculating the covariance matrix. The temperature in the slow-exchange regimes was calibrated with a methanol thermometer (*13*) and a 10-mm NMR dual-tube assembly in which the outer tube contained undiluted methanol and the inner tube contained the sealed methylcyclohexane solution. The chemical shifts were found to be linear in temperature, and the correlation of the chemical shift difference between the equatorial C-Me and C-2,6 spectral lines was used to measure the temperature in other low-temperature experiments. The dual-tube assembly was used to directly measure the temperature in the intermediate- and fast-exchange regions. The spectrometer response was found to be linear under similar operating conditions by using a solution of methylcyclohexane (major conformation) in cyclohexane under concentrations that were approximately equal to the major and minor conformers. The filter response of the spectrometer was measured, and intensity corrections of up to 3% were measured and applied to the outermost resonances. Spin-lattice relaxation times T_1 for the proton magnetization varied from 0.3 to 0.55 s at 180 K to 0.14 to 0.25 s at 143 K. Relaxation delays between scans were varied between 2 and 8 s.

17. This measurement of the free energy is consistent with an earlier measurement of $\Delta A_0 = 6317 \pm 837$ J mol^{-1} and $d\Delta A(T)/dT = 6.7 \pm 5.4$ J mol^{-1} K^{-1} (*8, 14*) but is more precise.
18. Linearity of the temperature dependence of the chemical shifts with respect to a cyclohexane reference was previously reported for the conformers of methylcyclohexane and for the related compounds *cis-* and *trans-*1,4-dimethylcyclohexane, where the chemical shifts are linear over the entire measured region of 70 K for the cis conformation and 120 K for the trans conformation (*14*).
19. P. R. Bevington, *Data Reduction and Error Analysis for the Physical Sciences* (McGraw-Hill, New York, ed. 1, 1969). The extent to which the reduced χ^2 is >1 allows a quantitation of the probability that the observed deviations of the data from the best fit are consistent with the random experimental errors, the determination of which is described in the caption of Fig. 2. For the global fits presented here, 225 data points are included: 57 for the slow-exchange equilibrium constants, 16 for the fast-exchange averages, and 152 for the slow-exchange chemical shifts of the major and minor conformers.
20. A conceivable systematic error would be caused by the neglect of a hypothetical third conformer, which might be present at undetectable levels in slow exchange but would contribute significantly in fast exchange. Cryogenic trapping experiments on methylcyclohexane from an initial temperature of 873 K (*15*) set an upper bound at 300 K of 10^{-4} for the ratio of a hypothetical third conformer to that of the equatorial form, whereas a population of several percent would be needed to account for the present observations with reasonable chemical shift parameters.
21. C. Cohen-Tannoudji, J. Dupont-Roc, G. Grynberg, *Atom-Photon Interactions: Basic Processes and Applications* (Wiley, New York, 1992).
22. L. J. Mueller, thesis, California Institute of Technology, Pasadena (1997); L. J. Mueller and D. P. Weitekamp, in preparation.
23. These contributions to the unitary evolution may be viewed as resulting from ALBATROSS. The description of the spectral densities in terms of system and bath susceptibilities (*21*) is not elaborated here.

24. This work was supported by NSF (grant CHE-9005964). L.J.M. acknowledges an NSF Graduate Fellowship and a Department of Defense National Defense Science and Engineering Graduate Fellowship.

30 April 1998; accepted 16 November 1998

Chain Length Recognition: Core-Shell Supramolecular Assembly from Oppositely Charged Block Copolymers

Atsushi Harada and Kazunori Kataoka*

Molecular recognition based on length was found to occur between oppositely charged pairs of flexible and randomly coiled block copolymers in an aqueous milieu. Matched pairs with the same block lengths of polyanions and polycations exclusively formed even in mixtures with different block lengths. These assemblies of the charged segments with matched chain lengths then formed larger core-shell–type supramolecular assemblies with an extremely narrow size distribution due to the strict phase separation between core- and shell-forming segments.

Recently, molecular recognition and the resulting supramolecular assembly processes have received considerable attention in chemistry, biology, and applied fields. Carefully designed chemical architectures promote precise molecular recognition, often leading to an assembly process (*1–6*). A common strategy for the formation of supramolecular assemblies is the construction of spatially ordered networks of noncovalently bonded constituent molecules. Most of studies in this area to date have been focused on the design of spatially ordered structures in which small differences in the steric factors of the constituent molecules crucially affect the thermodynamic stability and assembly of the system (*7*). Here we introduce a molecular recognition system that uses assembly of coiled block copolymers. Exclusive pairwise recognition of oppositely charged polymer strands occurs selectively on the basis of length, creating multimolecular micellization of pairs of oppositely charged block copolymers in aqueous solution. The block copolymers used here were composed of oppositely charged pairs of poly(ethylene glycol)-b-poly(α,β-aspartic acid) (Scheme 1)

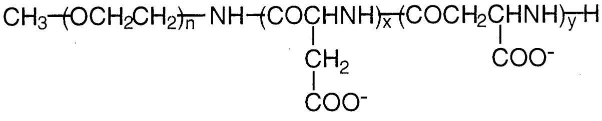

$$\mathrm{CH_3{-}(OCH_2CH_2)_n{-}NH{-}(CO\underset{\begin{array}{c}|\\ CH_2\\ |\\ COO^-\end{array}}{CH}NH)_x{-}(COCH_2\underset{\begin{array}{c}|\\ COO^-\end{array}}{CH}NH)_y{-}H}$$

Scheme 1

and poly(ethylene glycol)-b-poly(L-lysine) (Scheme 2)

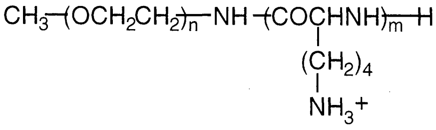

$$\mathrm{CH_3{-}(OCH_2CH_2)_n{-}NH{-}(CO\underset{\begin{array}{c}|\\ (CH_2)_4\\ |\\ NH_3^+\end{array}}{CH}NH)_m{-}H}$$

Scheme 2

We reported previously that mixing this pair of block copolymers with the same degree of polymerization (DP) in aqueous media led to the spontaneous formation of polyion complex (PIC) micelles having diameters of several tens of nanometers with an extremely narrow size distribution (*8*). A core-shell architecture with the PIC core surrounded by a poly(ethylene glycol) (PEG) corona was proposed for these PIC micelles.

Block copolymers were synthesized by the ring-opening polymerization of *N*-carboxyanhydride of the amino acids β-benzyl-L-aspartate or ε-benzyloxycarbonyl-L-lysine, initiating from the ω-NH_2 group of α-methoxy-ω-aminopoly(ethylene glycol) (*8*). The molecular weight (M_w) of the PEG segment was fixed at 5000 g/mol for all block copolymers examined in this study. After polymerization, protecting groups on the poly(amino acid) segments were removed either by alkali treatment (β-benzyl-L-aspartate) or by acid treatment (ε-benzyloxycarbonyl-L-lysine). Block copolymers thus obtained were confirmed to have a fairly narrow M_w distribution [ratio of the weight-averaged to number-averaged molecular weight (M_w/M_n) < 1.10] by gel filtration chromatography (GFC). For both anionic and cationic partners, two sets of copolymers with different DP of poly(amino acid) segments (18 and 78) were prepared and were abbreviated as A-18 and A-78 (Scheme 1) and as C-18 and C-78 (Scheme 2), respectively.

Recognition and selectivities for specific chain lengths upon micellization were directly monitored by GFC (Fig. 1). Gel filtration of the 1:1 mixture of the anionic polymers A-18 and A-78 [based on the aspartic acid (Asp) content]

Department of Materials Science, Graduate School of Engineering, University of Tokyo, 7-3-1 Hongo, Bunkyo-ku, Tokyo 113-8656, Japan.

*To whom correspondence should be addressed.